Journal of Solid State Chemistry 183 (2010) 1715–1720

Contents lists available at ScienceDirect

Journal of Solid State Chemistry

journal homepage: www.elsevier.com/locate/jssc

Synthesis, photophysical and oxygen-sensing properties of a novel Eu^{3+} complex incorporated in mesoporous MCM-41

Qinghui Zuo [a,b], Bin Li [a,*], Liming Zhang [a,b], Yinghui Wang [a,b], Yanhong Liu [a,b], Jun Zhang [c], Ying Chen [c], Lifan Guo [c]

[a] *Key Laboratory of Excited State Processes, Changchun Institute of Optics, Fine Mechanics and Physics, Chinese Academy of Sciences, Changchun 130033, PR China*
[b] *Graduate School of the Chinese Academy of Sciences, Chinese Academy of Sciences, Beijing 100039, PR China*
[c] *Polyoxometalate Science Key Laboratory of Ministry of Education, Department of Chemistry, Northeast Normal University, Changchun 130024, PR China*

ARTICLE INFO

Article history:
Received 28 January 2010
Received in revised form
30 April 2010
Accepted 20 May 2010
Available online 27 May 2010

Keywords:
Mesoporous composites
Eu^{3+} complex
Oxygen-sensing properties

ABSTRACT

A novel Eu^{3+} complex of Eu(DPIQ)(TTA)$_3$ (DPIQ=10H-dipyrido [*f*,*h*] indolo [3,2-*b*] quinoxaline, TTA=2-thenoyltrifluoroacetonate) was synthesized and encapsulated in the mesoporous MCM-41, hoping to explore an oxygen-sensing system based on the long-lived Eu^{3+} emitter. The Eu(DPIQ)(TTA)$_3$/MCM-41 composites were characterized by infrared spectra (IR), ultraviolet-visible (UV–vis) absorption spectra, small-angle X-ray diffraction (SAXRD), luminescence intensity quenching upon various oxygen concentrations, and fluorescence decay analysis. The results indicated that the composites exhibited the characteristic emission of the Eu^{3+} ion and the fluorescence intensity of $^5D_0$–$^7F_2$ obviously decreased with increasing oxygen concentrations. The oxygen sensing properties of the composites with different loading levels of Eu(DPIQ)(TTA)$_3$ complex were investigated. A sensitivity of 3.04, a short response time of 7 s, and good linearity were obtained for the composites with a loading level of 20 mg/g. These results are the best reported values for optical oxygen-sensing materials based on Eu^{3+} complexes so far.

1. Introduction

Oxygen is one of the most important chemical species for life. The determination of molecular oxygen is required in various fields of biochemical and clinical analyses as well as environmental monitoring. To date, the Clark electrode (CE) which is based on the electrochemical-reduction of oxygen on a polarized cathode has become the most traditionally used oxygen sensors [1]. However, the CE suffers some drawbacks, such as oxygen consumption during sensing process, relatively long response time, and the tendency of electrode to be poisoned by sample constituents (e.g., H_2S, proteins, and certain anesthetics) [2]. Given these limitations, researchers have expended substantial efforts to develop new techniques for oxygen detection. Among these techniques, optical oxygen sensors based on luminescence quenching are much more attractive due to the advantages of low cost, miniaturization, easy utilization, and not suffering from electrical interference or oxygen consumption [3].

Optical oxygen sensors are composed of organic dyes immobilized in oxygen permeable matrices. Many luminescent dyes have been developed as oxygen-sensing probes [4–7]. Probe molecules with high luminescence quantum yield, long fluorescence lifetime, and good photostability are desirable for optical oxygen sensors. Additionally, the properties of optical oxygen sensors depend on the structures of supporting matrices to a great extent. For example, a high gas diffusion coefficient is necessary for rapid response; a high locally quenching around the complex molecule is necessary for good sensitivity [6–8].

Eu^{3+} complexes, as important luminescent materials, have been widely applied in optical amplifications, light-conversion molecular devices (LCMD), organic light-emitting diodes (OLEDs), and other fields [9,10]. Recently, the luminescence properties of Eu^{3+} complexes supported on a stable matrix have been studied extensively because their photophysical properties could be modified by interaction with host structures [11–15]. Generally, several Eu^{3+} complexes display extremely sharp emission lines, intense luminescence with high quantum yields, and long fluorescence lifetimes [16]. Therefore, they are expected to be promising candidates as novel optical oxygen-sensing materials. However, only a few attempts have been made to use Eu^{3+} complexes as optical oxygen-sensing materials so far [17,18].

In this paper, we firstly synthesize a novel Eu^{3+} complex Eu(DPIQ)(TTA)$_3$, and encapsulate the Eu^{3+} complex into MCM-41. MCM-41 may provide a better support for the Eu^{3+} complex because of their large surface area, highly ordered and nearly parallel channel, which is necessary for higher sensitivity and

---

* Corresponding author. Fax: +86 431 86176935.
E-mail address: lib020@yahoo.cn (B. Li).

0022-4596/$ - see front matter © 2010 Elsevier Inc. All rights reserved.
doi:10.1016/j.jssc.2010.05.022

faster response time [19,20]. The oxygen sensing properties of the composites are investigated and the obtained values are found to be much better than those of other oxygen-sensing materials based on Eu^{3+} complexes.

2. Material and methods

2.1. Materials and reagents

Analytical grade solvents and compounds were used for preparation. Tetraethoxysilane (TEOS, Tianjin Chemicals Co.), cetyltrimethylammonium (CTAB, Aldrich), and ethanol (Tianjin Chemicals Co.) were used as received. The water used in our work was deionized. 1, 10-Phenanthroline monohydrate was obtained from Beijing Fine Chemical Company (Beijing, China). Concentrated HCl was obtained from Shanghai Chemical Company (Shanghai, China).

2.2. Synthesis procedures

2.2.1. Synthesis of DPIQ ligand

DPIQ was synthesized by modification according to the literatures [21,22]. Isatin (1 mmol, 0.147 g) was refluxed with 1, 10-phenanthroline-5, 6-diamine (1 mmol, 0.21 g) in 20 mL ethanol for more than 8 h until a suspension was formed. The mixture was hot filtered off to recuperate a pale yellow powder. The crude product subsequently was purified by recrystallization from methanol to give the desired product. ^1H NMR($CDCl_3$, 500 MHz): δ 10.07 (d, 1H, $J=8.5$ Hz), 9.22 (d, 1H, 2.5 Hz), 9.13 (d, 1H, 2.0 Hz), 9.05 (d, 1H, 5.5 Hz), 8.52 (d, 1H, 5.5 Hz), 7.62–7.72 (m, 2H), 7.57 (d, 1H, 8.5 Hz), 7.33 (m, 3H). IR (KBr pellets): 3414, 3048, 2986, 2812, 2754, 1720, 1601, 1566, 1375, 737 cm^{-1}. Anal. Calcd for $C_{20}H_{11}N_5$: C, 74.76; H, 3.43; N, 21.80. Found: C, 74.61; H, 3.21; N, 21.69.

2.2.2. Synthesis of $Eu(DPIQ)(TTA)_3$ complex

$Eu(DPIQ)(TTA)_3$ was synthesized according to a literature procedure [23]. (0.3 mmol, 0.067 g) HTTA and (0.1 mmol, 0.032 g) DPIQ was dissolved in 5 mL ethanol solution under stirring. Sodium hydroxide was added until pH value of the solution approached 7. Then (0.1 mmol, 0.037 g) $EuCl_3 \cdot 6H_2O$ in 2 mL water was added to the mixed solution. The mixture was stirred for 1 h at 60 °C. The product was collected by filtration and recrystallized from ethanol. IR (KBr pellets): 3425, 1714, 1600, 1537, 1407, 1351, 730, 501 cm^{-1}. Anal. Calcd. for $C_{44}H_{23}N_5F_9O_6S_3Eu$: C, 46.48; H, 2.04; N, 6.16. Found: C, 46.64; H, 1.86; N, 6.32.

2.2.3. Synthesis of $Eu(DPIQ)(TTA)_3$/MCM-41 composites

$Eu(DPIQ)(TTA)_3$/MCM-41 composites were prepared by a similar route as the literature [24]. In typical preparation, 10 mg $Eu(DPIQ)(TTA)_3$ was dissolved in 5 mL dichloromethane solution to form a light yellow transparent solution, then 1 g MCM-41 was added. The mixture was stirred for 5 h and filtered to give a yellowish power. The yellowish power was washed by dichloromethane for several times until the filtered dichloromethane solution was colorless under UV illumination, and dried in the air. 10 mg $Eu(DPIQ)(TTA)_3$/g MCM-41 was obtained. The composites with different loading levels of $Eu(DPIQ)(TTA)_3$ (20 and 30 mg $Eu(DPIQ)(TTA)_3$/g MCM-41) were prepared by altering the concentration of the starting solution of $Eu(DPIQ)(TTA)_3$.

2.3. Characterization

The ^1H NMR spectra were recorded on a Bruker DPX-300 NMR spectrometer. The infrared spectra were measured using a Magna560 FT-IR spectrophotometer. The elemental analysis was obtained using a Vario Element Analyzer. The SAXRD spectra were reported on a Siemens D5005 diffractometer. The UV–vis absorption spectra were obtained using a Cary 500 Scan UV–vis-NIR Spectrophotometer. The fluorescence decay analysis was carried out using a Nd:YAG (neodymium yttrium aluminum garnet) laser system (Spectra Physics). Luminescence spectra were obtained using a Hitachi F-4500 fluorescence spectrophotometer. For the Stern–Volmer plot measurements, oxygen and nitrogen were mixed at different concentration via gas flow controls and passed directly to the sealed gas chamber.

3. Results and discussion

3.1. Synthesis and characterization

The DPIQ and $Eu(DPIQ)(TTA)_3$ were synthesized as the literature methods [21–23]. Their composition and purity were confirmed by ^1H NMR, IR spectroscopy and elemental analysis. The structure of $Eu(DPIQ)(TTA)_3$ was depicted in Fig. 1.

Infrared spectra of DPIQ, TTA, $Eu(DPIQ)(TTA)_3$, and $Eu(DPIQ)(TTA)_3$/MCM-41 composites with different loading levels of Eu^{3+} complexes are shown in Fig. 2a and b. As shown in Fig. 2a, the IR spectra show a displacement of stretching vibration of C=O from 1654 cm^{-1} in free HTTA to 1600 cm^{-1} in the Eu^{3+} complex, and a displacement of stretching vibration of C=N from 1375 cm^{-1} in the free DPIQ to 1351 cm^{-1} in the Eu^{3+} complex, indicating that the Eu^{3+} ion is coordinated through oxygen and nitrogen atoms [25]. In Fig. 2b, the symmetric vibration peak of Si–O–Si is moved from 814 (pure MCM-41) to 808 cm^{-1} (samples A, B, and C), revealing that $Eu(DPIQ)(TTA)_3$ complexes have been contained in MCM-41 [26]. In addition, a number of sharp vibration peaks appear in the range of 560–840 and 1000–1750 cm^{-1} for the $Eu(DPIQ)(TTA)_3$/MCM-41 complexes, whereas they do not appear in the $Eu(DPIQ)(TTA)_3$/MCM-41 composites, which suggests the pure complexes were actually incorporated into MCM-41 channels but not physically absorbed outside [11].

3.2. UV–vis absorption spectra and fluorescence properties

The UV–vis absorption spectra of TTA, DPIQ, $Eu(DPIQ)(TTA)_3$, and $Eu(DPIQ)(TTA)_3$/MCM-41 composites with different loading levels of Eu^{3+} complexes in dichloromethane solution are drawn in Fig. 3. As for pure $Eu(DPIQ)(TTA)_3$, two absorption bands located around 225 and 279 nm are observed, corresponding to the π–π^* electronic transitions of DPIQ [27,28]. The band at 336 nm is assigned to the absorption of TTA electronic transitions. The absorption feature of $Eu(DPIQ)(TTA)_3$/MCM-41 composites is consistent with that of the pure $Eu(DPIQ)(TTA)_3$ dissolved in dichloromethane solution, indicating that $Eu(DPIQ)(TTA)_3$ has been dispersed in the channels of MCM-41. For the composite with a loading level of 10 mg/g, the absorption bands are very weak because of the low concentration of Eu^{3+} complexes [12].

The emission spectra of $Eu(DPIQ)(TTA)_3$ in the air, pure nitrogen, and pure oxygen and amplified part of emission spectra are shown in Fig. 4a and b. As shown in Fig. 4a, $Eu(DPIQ)(TTA)_3$ exhibits characteristic emission of Eu^{3+} ion, and the hypersensitive $\Delta J=2$ transition gives rise to the greatest changes in the Eu^{3+} emissions in pure oxygen, compared to that in the air and pure nitrogen. Again, the Eu^{3+} emissions at 578,

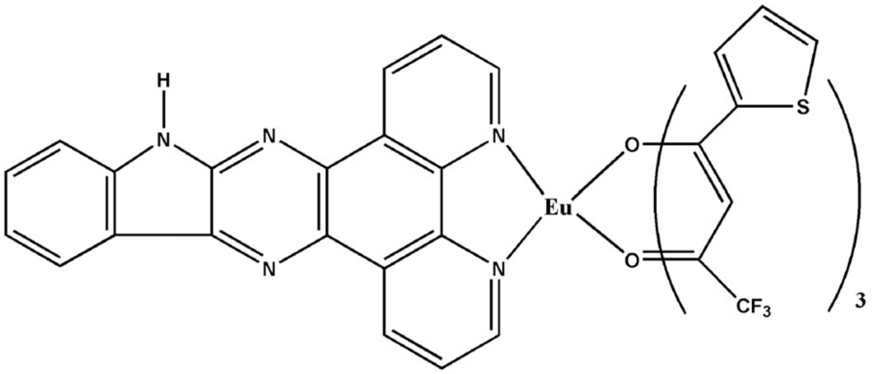

Fig. 1. Molecular structure of Eu(DPIQ)(TTA)$_3$.

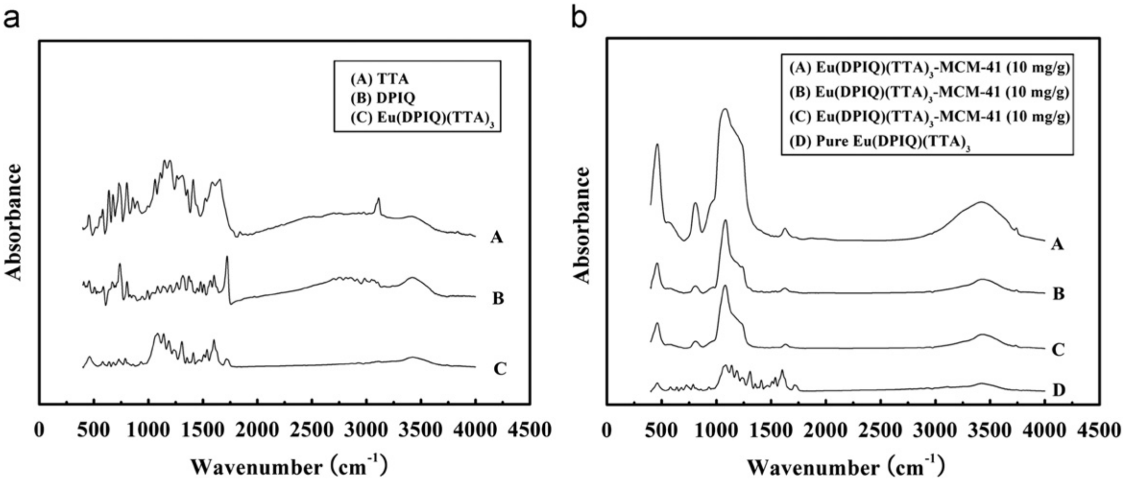

Fig. 2. (a) IR spectra of DPIQ, TTA, and Eu(DPIQ)(TTA)$_3$. (b) IR spectra of Eu(DPIQ)(TTA)$_3$ and Eu(DPIQ)(TTA)$_3$/MCM-41 composites with different loading levels of Eu^{3+} complexes.

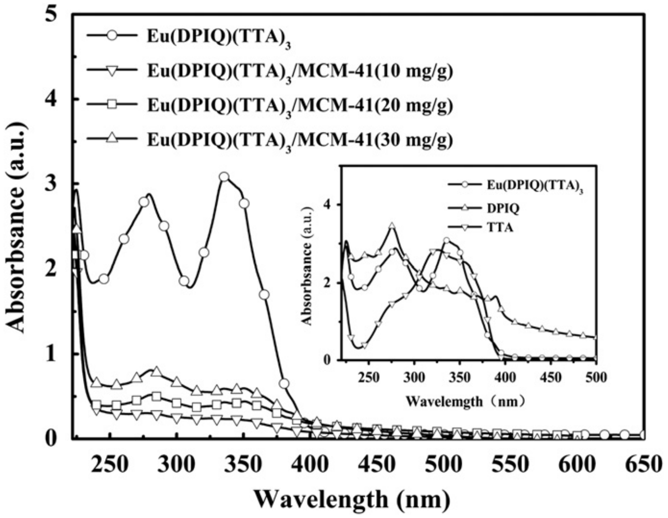

Fig. 3. UV–vis absorption spectra of TTA, DPIQ, Eu(DPIQ)(TTA)$_3$, and Eu(DPIQ)(TTA)$_3$/MCM-41 composites with different loading levels of Eu^{3+} complexes in dichloromethane solution with a concentration of 1×10^{-5} mol/L.

590, 650, and 699 nm (for $^5D_0\rightarrow{}^7F_J$ (J=0, 1, 3, and 4)) also decrease with increasing oxygen concentrations, as shown in Fig. 4b. This demonstrates the Eu^{3+} emissions could be effectively quenched by oxygen. The fluorescence decay time curve of $^5D_0$–$^7F_2$ transition for Eu^{3+} ion in the pure Eu(DPIQ)(TTA)$_3$ complex is shown in Fig. 5. It can be seen that the $^5D_0$–$^7F_2$ transition follows an exponentially decay with a lifetime of 300 μs.

3.3. Oxygen-sensing properties

The SAXRD patterns of pure MCM-41 and Eu(DPIQ)(TTA)$_3$/MCM-41 composites with different loading levels of Eu(DPIQ)(TTA)$_3$ complex are shown in Fig. 6. All composites exhibit three degree intense broad Bragg reflections that could be indexed as d_{100}, d_{110}, d_{200}, confirming the nature of a highly ordered hexagonal mesostructure. The presence of the three diffraction peaks indicates the ordered hexagonal mesoporous structure of MCM-41 remains intact after the introduction of Eu(DPIQ)(TTA)$_3$. These results combined with above mentioned IR and UV–vis absorption spectra further confirm that Eu(DPIQ)(TTA)$_3$ complexes are successfully incorporated into MCM-41channels.

The emission spectra of Eu(DPIQ)(TTA)$_3$/MCM-41 composites with different loading levels of Eu(DPIQ)(TTA)$_3$ complex under different oxygen concentrations are presented in Fig. 7. It can be seen that the emission intensity of $^5D_0$–$^7F_2$ transition for Eu^{3+} ion in all samples decreases obviously with increasing oxygen concentrations. Therefore, Eu(DPIQ)(TTA)$_3$/MCM-41 composites could be exploited as optical oxygen-sensing materials.

The quenching behavior of luminescent molecules is affected by the microstructure of matrix and the micro-environment in which the molecules are located [29,30]. In a homogeneous

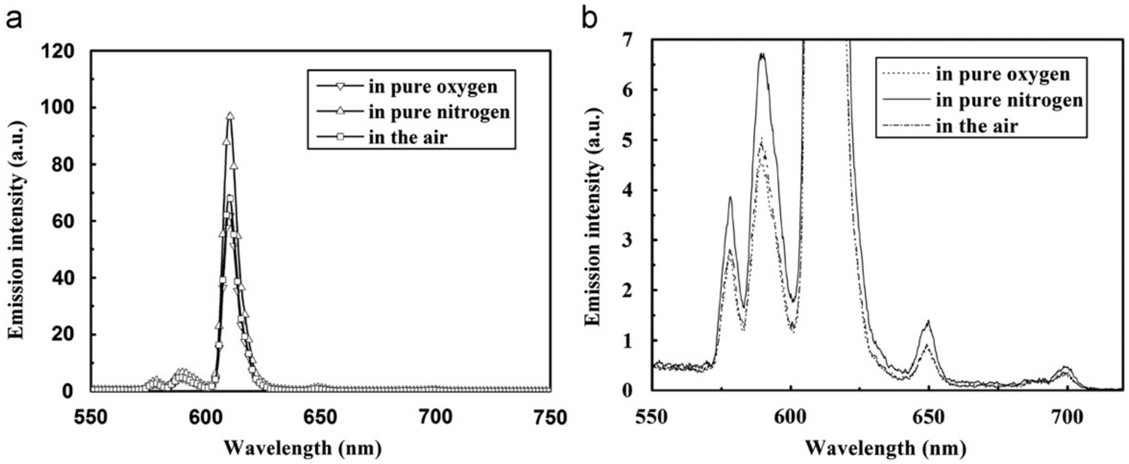

Fig. 4. (a) Solid-state emission spectra of Eu(DPIQ)(TTA)$_3$ in the air, pure nitrogen, and pure oxygen. $\lambda_{ex}=365$ nm. (b) Amplified part of solid-state emission spectra of Eu(DPIQ)(TTA)$_3$.

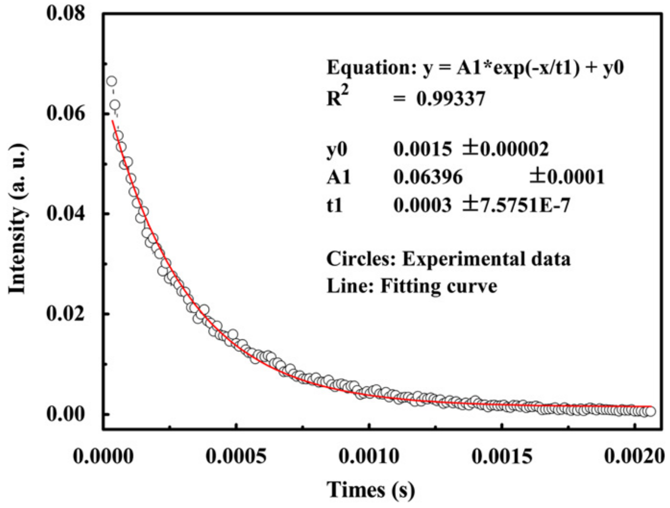

Fig. 5. Solid-state fluorescence lifetime decay curve of the $^5D_0$–$^7F_2$ transition of Eu(DPIQ)(TTA)$_3$ at 610 nm in the air.

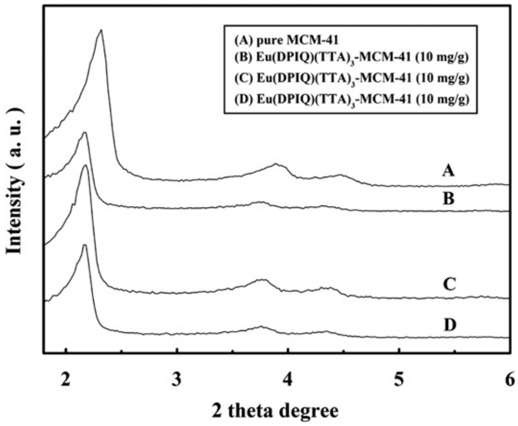

Fig. 6. SAXRD diffraction patterns of pure MCM-41 and Eu(DPIQ)(TTA)$_3$/MCM-41 composites with the loading levels of 10, 20, and 30 mg/g.

medium with a single-exponential decay, the luminescent intensity and decay lifetime with oxygen concentration can be described by the Stern–Volmer equation as follows:

$$I_0/I=\tau_0/\tau=1+K_{SV}[O_2]=1+K_q\tau_0[O_2] \tag{1}$$

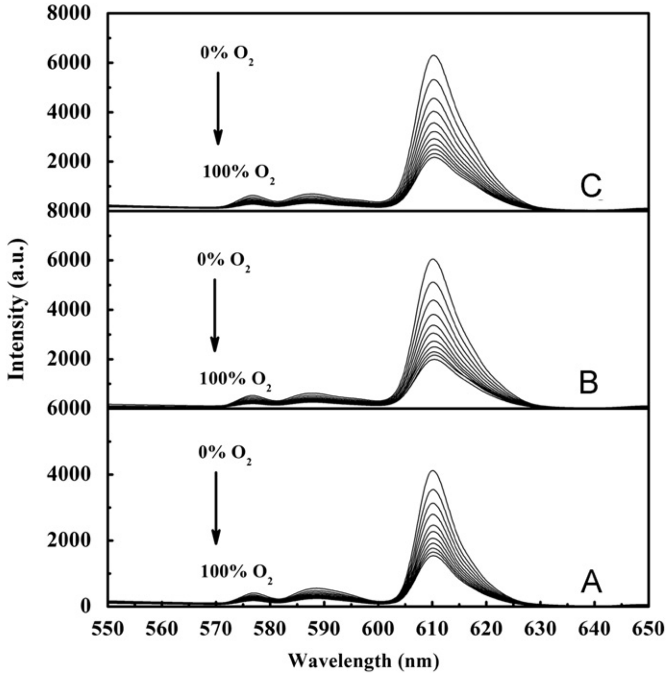

Fig. 7. Emission spectra of Eu(DPIQ)(TTA)$_3$/MCM-41 composites at different oxygen concentrations: (A) 10, (B) 20, and (C) 30 mg/g. $\lambda_{ex}=365$ nm.

where I and τ are the luminescent intensity and decay lifetime of the luminophore, respectively. The subscript 0 denotes the absence of oxygen. K_{SV} is the Stern–Volmer constant, K_q is the bimolecular quenching constant, and $[O_2]$ is the O_2 concentration. A plot of I_0/I or τ_0/τ versus $[O_2]$ should be linear with identical slopes of K_{SV}. The fluorescent decay lifetime of luminophore in a homogeneous medium can be described by a single-exponential equation [29,31]

$$I(t)=\alpha\exp(-t/\tau) \tag{2}$$

where $I(t)$ is the luminescence intensity at time t and α is the pre-exponential factor.

Fig. 8 presents the Stern–Volmer plots for Eu(DPIQ)(TTA)$_3$/MCM-41 composites (10, 20, and 30 mg/g) at different oxygen concentrations. The intensity-based Stern–Volmer oxygen-quenching fitting parameters are complied in Table 2. Inspection of these results reveals two key points. First, the Stern–Volmer plots for the composites with different loading levels of

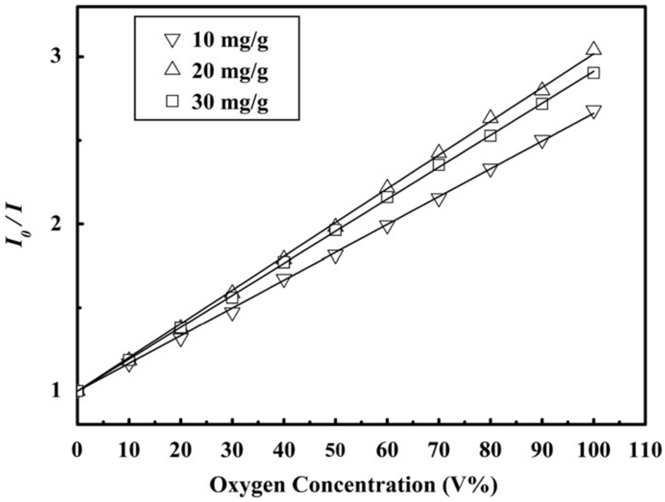

Fig. 8. Stern–Volmer plots of Eu(DPIQ)(TTA)$_3$/MCM-41 composites with the loading levels of 10, 20, and 30 mg/g at different oxygen concentrations.

Table 1
Fluorescent decay constants of Eu(DPIQ)(TTA)$_3$/MCM-41 composites with the loading levels of 10 (A), 20 (B), and 30 mg/g (C) in the air, pure nitrogen, and pure oxygen.

Samples	Gas	α	τ (μs)	R^2
A	N_2	0.14422 ± 0.00024	450	0.9939
	Air	0.1252 ± 0.00021	310	0.9968
	O_2	0.0715 ± 0.00021	190	0.9953
B	N_2	0.01001 ± 0.00022	590	0.9972
	Air	0.16027 ± 0.00019	430	0.9975
	O_2	0.06858 ± 0.00017	270	0.9951
C	N_2	0.25754 ± 0.00028	590	0.9970
	Air	0.18081 ± 0.00024	430	0.9970
	O_2	0.09447 ± 0.00014	400	0.9969

Eu(DPIQ)(TTA)$_3$ complex exhibit an excellent linear relationship and are reasonably well described by Eq. (1). These results demonstrate the micro-environment surrounding Eu(DPIQ)(TTA)$_3$ molecules within Eu(DPIQ)(TTA)$_3$/MCM-41 composites is homogeneous [32]. Second, the composite with a loading level of 20 mg/g exhibits a sensitivity of 3.04 which is superior to those of samples with loading levels of 10 and 30 mg/g. It may be interpreted as follows: the sensitivity of the composites initially increases, suggesting that the quenching between oxygen and luminophore molecules become more effective with increasing Eu(DPIQ)(TTA)$_3$ concentration. When the concentration of Eu(DPIQ)(TTA)$_3$ changes from 20 to 30 mg/g, the sensitivity decreases due to the adverse intermolecular interaction existed between luminophore molecules in the pores of MCM-41 [7].

To further explain the sensing mechanism of Eu(DPIQ)(TTA)$_3$/MCM-41 composites, fluorescence decay lifetimes of $^5D_0$–$^7F_2$ transition for Eu(DPIQ)(TTA)$_3$/MCM-41 composites (10, 20, and 30 mg/g) in pure oxygen, the air and pure nitrogen are studied. Fluorescence decay constants are listed in Table 1. The data can be fitted by Eq. (2). The studies disclose that the fluorescence decay lifetimes of Eu(DPIQ)(TTA)$_3$/MCM-41 composites depend on oxygen concentration. Thus, a dynamic quenching mechanism [33] may be responsible for the fluorescence quenching. The sensing mechanism of Eu(DPIQ)(TTA)$_3$/MCM-41 composites can be described as follows:

$$Eu(III)^{*}+O_2 \rightarrow Eu(III)+O_2^{*}$$

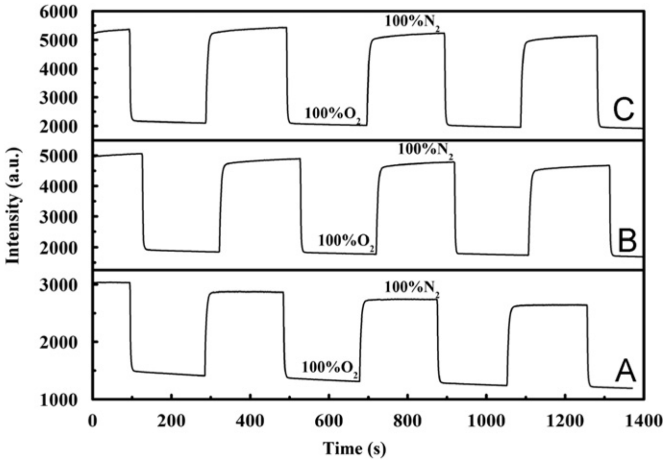

Fig. 9. Response time, relative intensity change of Eu(DPIQ)(TTA)$_3$/MCM-41 composites with the loading levels of 10 (A), 20 (B), and 30 mg/g (C) at 610 nm on periodically cycling from 100% nitrogen to 100% oxygen.

It is well known that the luminescence of Eu^{3+} complexes is attributed to the electronic transitions from $^5D_0$ excited state to ^7F_n ground state. In the present of oxygen, a large part of excited-state energy is transferred to ground state oxygen, leading to the $^5D_0$–^7F_n luminescence quenching.

Fig. 9 demonstrates the typical dynamic response of the composites with different loading levels of Eu^{3+} complexes upon exposure to 100% nitrogen and 100% oxygen atmospheres which are varied periodically. From the response time plots, the 95% response ($t_{\downarrow}$) and 95% recovery ($t_{\uparrow}$) time to an alternating atmosphere of 100% nitrogen and 100% oxygen can be calculated. Generally, $t_{\downarrow}$ and $t_{\uparrow}$ are defined as the time taken for a sample to attain 95% of its total emission intensity change when the gas is changed from 100% nitrogen to 100% oxygen and from 100% oxygen to 100% nitrogen, respectively. The values of $t_{\downarrow}$, $t_{\uparrow}$ and sensitivity are listed in Table 2. As shown in Fig. 9, all composites exhibit fully reversible time response plots, and no drift intensity is founded. The sensor response is stable and very fast, owing to the highly ordered channels of MCM-41 matrix, which facilitates the high diffusion of gas. The stable and reversible response signals indicate that Eu(DPIQ)(TTA)$_3$/MCM-41 composites possess an excellent photostability.

The average sensitivity and response stability of the composites at 15 and 30 °C over three months have been measured. The results deviation is small enough to be neglected, indicating that Eu(DPIQ)(TTA)$_3$/MCM-41 composites are stable over temperature and time. Therefore, they could be used as optical oxygen-sensing materials because of their good sensitivity, fast response, and high photostability.

4. Conclusions

Novel optical oxygen-sensing composites are prepared by incorporating the Eu^{3+} complex Eu(DPIQ)(TTA)$_3$ into MCM-41. The oxygen sensing properties of the composites with different loading levels of Eu(DPIQ)(TTA)$_3$ complex are systemically studied. The luminescence of Eu(DPIQ)(TTA)$_3$/MCM-41 composites exhibits a strong oxygen dependent characteristic. The composite with a loading level of 20 mg/g possesses a good sensitivity of 3.04, a short response time of 7 s and an excellent linear relationship.

Table 2
Values of $t_{\downarrow}$, $t_{\uparrow}$, sensitivity (I_0/I_{100}) and intensity-based Stern–Volmer oxygen-quenching fitting parameters for Eu(DPIQ)(TTA)$_3$/MCM-41composites.

Loading levels (mg/g)	$t_{\downarrow}$ (s)	$t_{\uparrow}$ (s)	I_0/I_{100}	$K_{SV}(O_2\%^{-1})$	R^2
10	6	9	2.68	0.01662 ± 0.00007	0.99945
20	7	13	3.04	0.02018 ± 0.0001	0.99919
30	8	14	2.90	0.01913 ± 0.00004	0.99981

Acknowledgments

The authors gratefully thank the financial supports of One Hundred Talents Project from the Chinese Academy of Sciences and the NSFC (Grant no. 50872130).

References

[1] L.C. Clark Jr., Trans. Am. Soc. Artif. Intern. Organs 2 (1956) 41.
[2] J.R. Bacon, J.N. Demas, Anal. Chem. 59 (1987) 2780.
[3] Y. Amao, Microchim. Acta. 143 (2003) 1.
[4] W.Y. Xu, K.A. Kneas, J.N. Demas, B.A. DeGraff, Anal. Chem. 68 (1996) 2605.
[5] Y. Amao, Y. Ishikawa, I. Okura, Anal. Chim. Acta. 445 (2001) 177.
[6] B.F. Lei, H.R. Zhang, S.Z. Lu, Z.H. Zheng, W.L. Li, Y. Wang, Adv. Funct. Mater. 16 (2006) 1883.
[7] L.F. Shi, B. Li, S.M. Yue, D. Fan, Sensors Actuators B 137 (2009) 386.
[8] W.Y. Xu, R.C. McDonough, B. Langsdorf, J.N. Demas, B.A. DeGraff, Anal. Chem. 66 (1994) 4133.
[9] C.D.M. Donega, S.A. Junior, G.F.D. Sa, Chem. Commun. 16 (1996) 1199.
[10] P.P. Sun, J.P. Duan, H.T. Shih, C.H. Cheng, Appl. Phys. Lett. 81 (2002) 792.
[11] S.W. Li, H.W. Song, W.L. Li, X.G. Ren, S.Z. Lu, G.H. Pan, L.B. Fan, H.Q. Yu, H. Zhang, R.F. Qin, Q.L. Dai, T. Wang, J. Phys. Chem. B 110 (2006) 23164.
[12] Q.H. Xu, L.S. Li, X.S. Liu, R.R. Xu, Chem. Mater. 14 (2002) 549.
[13] B. Yan, Q.H. Wang, Cryst. Growth Des. 8 (2008) 1484.
[14] Y. Li, B. Yan, J. Solid State Chem. 181 (2008) 1032.
[15] L.L. Kong, B. Yan, Y. Li, J. Solid State Chem. 182 (2009) 1631.
[16] G. Vicentini, L.B. Zinner, J. Zukerman-Schpector, K. Zinner, Coord. Chem. Rev. 196 (2000) 353.
[17] Y. Amao, I. Okura, T. Miyashita, Bull. Chem. Soc. Jpn. 73 (2000) 2663.
[18] Y. Amao, I. Okura, T. Miyashita, Chem. Lett. Jpn. 29 (2000) 934.
[19] G. Wirnsberger, B.J. Scott, G.D. Stucky, Chem. Commun. 21 (2001) 119.
[20] A.B. Descalzo, D. Jimenez, M.D. Marcos, R. Martinez-Manez, J. Soto, J.E. Haskouri, C. Guillem, D. Beltran, P. Amoros, M.V. Borrachero, Adv. Mater. 14 (2002) 966.
[21] S. Bodige, F.M. MacDonnell, Tetrahedron Lett. 38 (1997) 8159.
[22] J. Bolger, A. Gourdon, E. Ishow, J.P. Launay, Inorg. Chem. 35 (1996) 2937.
[23] H. Bauer, J. Blanc, D.L. Ross, J. Am. Chem. Soc. 86 (1964) 5125.
[24] H.D. Zhang, Y.H. Sun, K.Q. Ye, P. Zhang, Y. Wang, J. Mater. Chem. 15 (2005) 3181.
[25] O.L. Malta, H.F. Brito, J.F.S. Menezes, F.R. Goncalves e Sulva, S. Alves Jr., F.S. Farias Jr., A.V.M. de Andrade, J. Lumin. 75 (1997) 255.
[26] M.D. Alba, Z.H. Luan, J. Klinowski, J. Phys. Chem. 100 (1996) 2178.
[27] E.B. van der Tol, H.J. van Ramesdonk, J.W. Verhoeven, F.J. Steemers, E.G. Kerver, W. Verboom, D.N. Reinhoudt, Chem. Eur. J. 4 (1998) 2315.
[28] X.N. Li, Z.J. Wu, Z.J. Si, L. Zhou, X.J. Liu, H.J. Zhang, Phys. Chem. Chem. Phys. 11 (2009) 9687.
[29] M.T. Murtagh, M.R. Shahriari, M. Krihak, Chem. Mater. 10 (1998) 3862.
[30] X. Chen, Z.M. Zhong, Z. Li, Y.Q. Jiang, X.R. Wang, K.Y. Wong, Sensors Actuators B 87 (2002) 233.
[31] E.R. Carraway, J.N. Demas, B.A. DeGraff, J.R. Bacon, Anal. Chem. 63 (1991) 337.
[32] Y. Tang, E.C. Tehan, Z. Tao, F.V. Bright, Anal. Chem. 75 (2003) 2407.
[33] B. Valeur, Wiley-VCH Verlag GmbH (2002) 72.